Supplementary Information for

Incorporation of a boryl pendant as the trigger in a methacrylate polymer for backbone degradation

Hiroshi Makino, Tsuyoshi Nishikawa* and Makoto Ouchi*

Department of Polymer Chemistry, Graduate School of Engineering, Kyoto University, Kyoto 606-8501, Japan

615-8510, Japan

*To whom correspondence should be addressed.

E-mail: nishikawa.tsuyoshi.8n@kyoto-u.ac.jp
ouchi.makoto.2v@kyoto-u.ac.jp

Contents

1 General

All reactions were carried out with magnetic stirring under a nitrogen or an argon atmosphere unless stated otherwise. ^{1}H NMR spectra were recorded on a JEOL JNM-ECA500 operating at 500.16 MHz (^{1}H) at ambient temperature. ^{1}H NMR data are reported on the basis of the chemical shift in ppm downfield from tetramethylsilane (δ scale). The number-average molecular weight (M_n), peak top molecular weight (M_p), and molecular weight distribution (M_w/M_n) of polymers were measured by HCL-8320GPC (TOSOH) at 40 °C in THF as an eluent on two polystyrene-gel columns (Shodex LF-404) at 0.35 mL/min of flow rate. The columns were calibrated against PMMA standard samples (PSS ReadyCal-Kit; Poly(methyl methacrylate), M_p = 800-2200000). Differential scanning calorimetry (DSC) was performed for polymer samples (ca. 3-6 mg in aluminum pan) under dry nitrogen flow on DSCQ200 calorimeter (TA Instruments) equipped with RCS 90 electric freezing machine. Heating and cooling of the samples were repeated at 10 ˚C/min between 0 ˚C and 150 ˚C and the data on the second heating was employed for the T_g evaluation. The second heating scans were employed as data in the work. Thermogravimetric analysis (TGA) of polymer samples (ca. 5-6 mg in aluminum pan) was performed under dry nitrogen flow on a STA 2500 *Regulus* (NETZSCH). Heating of the samples were repeated at 10 °C/min between 20 °C and 500 °C. T_{d5} was the temperature of 5% weight loss.
Vinylboronic acid pinacol ester (VBpin), isopropenylboronic acid pinacol ester (IPBpin), methyl methacrylate (MMA) and tetralin were purified by distillation prior to use. Azobisisobutyronitrile (AIBN), 2-Cyano-2-propyl dodecyl trithiocarbonate (CPDT), tetrabutylammonium fluoride trihydrate ($TBAF \cdot 3H_2O$), 4-*tert*-butylpyrocatechol (TBC), manganese(III) acetate dihydrate ($Mn(OAc)_3 \cdot 2H_2O$), *tert*-butylhydroquinone (TBHQ), 2,2,6,6-tetramethylpiperidine 1-oxyl (TEMPO) and dehydrated toluene were purchased from the commercial sources and were used without further purification.

2 Experimental Procedures

RAFT copolymerization of alkenylboronates with MMA

The typical procedure for the copolymerization of alkenylboronates with MMA is as follows. A toluene solution of AIBN (205 μL, 2.05 mg 12.5 μmol), tetralin (34.1 μL, 33.1 mg, 250 μmol, internal standard), CPDT (8.73 μL, 8.64 mg, 25.0 μmol), VBpin (107 μL, 96.3 mg, 630 mmol), MMA (466 μL, 438 mg, 4.38 mmol), and toluene (429 μL) were placed in a Schlenk tube having PTFE stopcock (J. Young) at room temperature under Ar ($[VBpin]_0/[MMA]_0/[CPDT]_0/[AIBN]$ = 500/3500/20/10 mM condition). The reaction solution was stirred at 60 °C in an oil bath. The polymerization solution was taken at predetermined intervals for analyses by SEC and ^{1}H NMR. Monomer conversion was determined by ^{1}H NMR from the peak area of olefinic protons of the monomer with tetralin as an internal standard. The polymer was purified by preparative SEC ($CHCl_3$ as eluent) and the degrees of polymerization of VBpin and MMA were analyzed by ^{1}H NMR. The copolymerization of IPBpin with MMA and homopolymerization of MMA were performed in the similar way.

Degradation of poly(alkenylboronate-*co*-MMA)

The typical procedure for degradation of poly(alkenylboronate-*co*-MMA) is as follows. Poly(VBpin-*co*-MMA) (50 mg, Bpin unit = 36.0 μmol), $TBAF \cdot 3H_2O$ (13.6 mg, 43.2 μmol),

$Mn(OAc)_3 \cdot 2H_2O$ (9.7 mg, 36.0 μmol), TBC (29.9 mg, 180 μmol), and toluene (511 μL) were placed in a Schlenk tube having PTFE stopcock (J. Young) at room temperature under Ar ([Bpin unit]$_0$/[TBAF]$_0$/[$Mn(OAc)_3$]$_0$/[TBC]$_0$ = 70/85/70/352 mM condition). The reaction solution was stirred at 120 °C in an oil bath for 24 h. The reaction was terminated by cooling to room temperature. The reaction mixture was diluted with $CHCl_3$, and washed with brine (5 mL × 3). The organic layer was filtered by aluminum oxide 90 active basic to remove Mn salt. The resultant solution was evaporated to remove solvents and the residue was analyzed by SEC.

3 Results of RAFT copolymerization

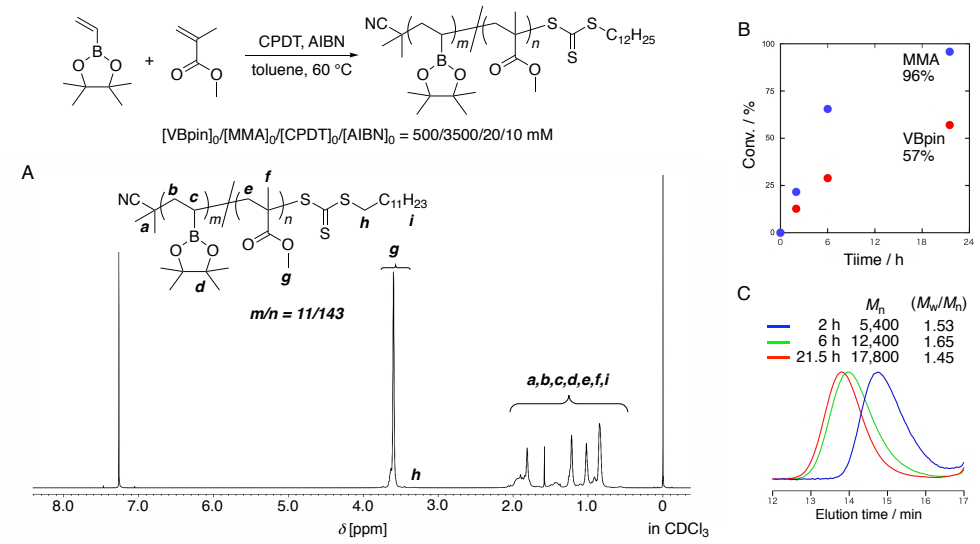

Figure S1. RAFT copolymerization of VBpin and MMA. (A) ^{1}H NMR spectrum of poly(VBpin-*co*-MMA) in $CDCl_3$ after purification. (B) Time-conversion curves. (C) Time-course SEC traces in the copolymerization.

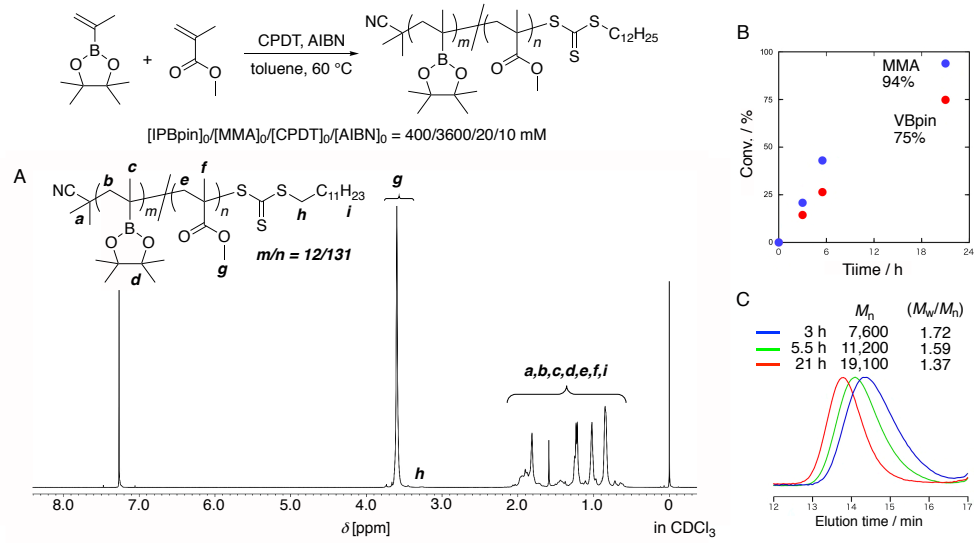

Figure S2. RAFT copolymerization of IPBpin and MMA. (A) ^{1}H NMR spectrum of poly(IPBpin-*co*-MMA) in $CDCl_3$ after purification. (B) Time-conversion curves. (C) Time-course SEC traces in copolymerization.

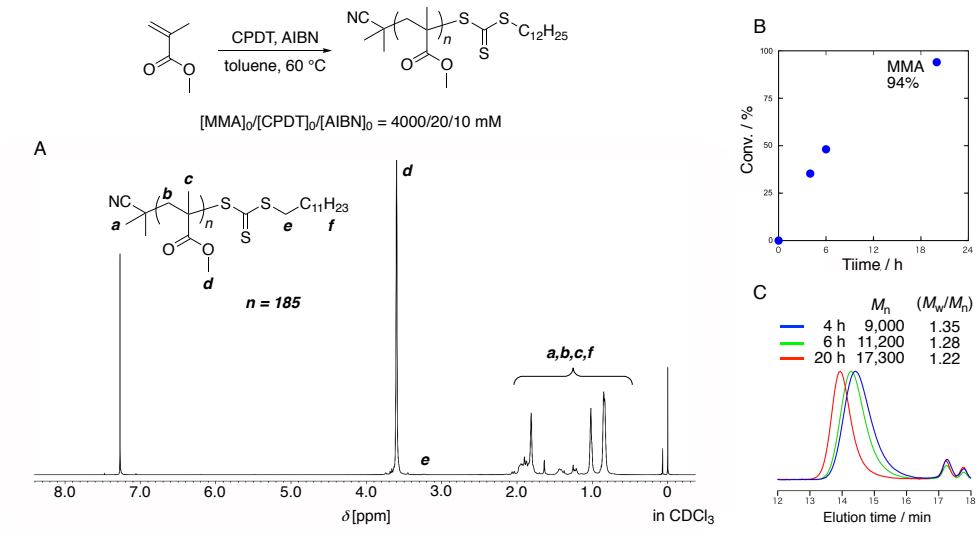

Figure S3. RAFT polymerization of MMA. (A) ^{1}H NMR spectrum of PMMA in $CDCl_3$ after purification. (B) Time-conversion curve. (C) Time-course SEC traces in copolymerization.

4 Results of Degradation of Poly(alkenylboronate-*co*-MMA)

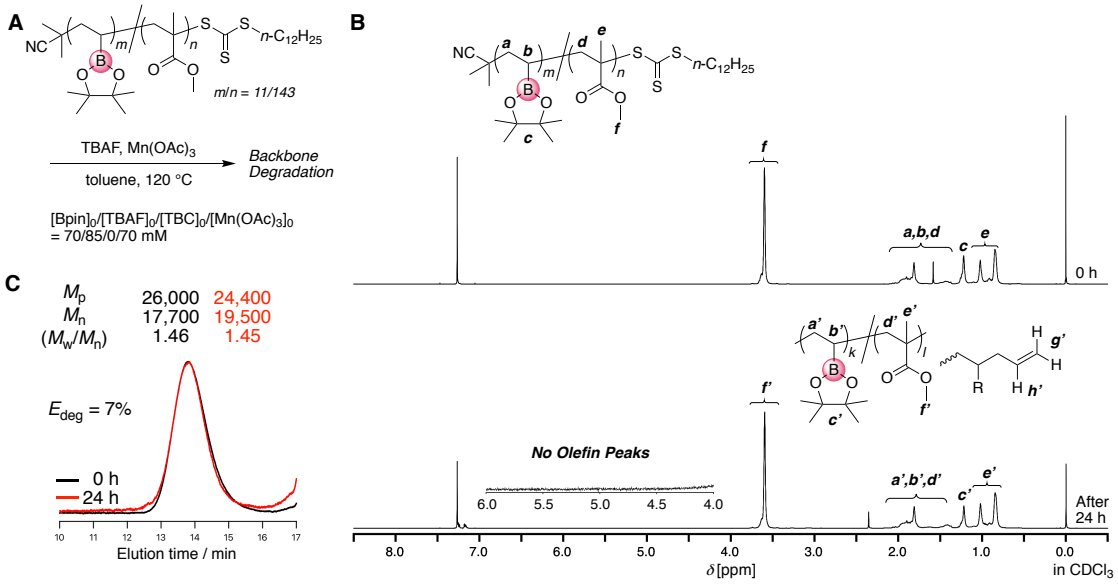

Figure S4. (A) Reaction condition for the degradation of poly(VBpin-*co*-MMA) (run 1 in Table 1). (B) ^{1}H NMR spectra of the precursor (upper) and the resultant polymer (bottom). (C) SEC traces of the precursor (black) and the resultant polymer (red).

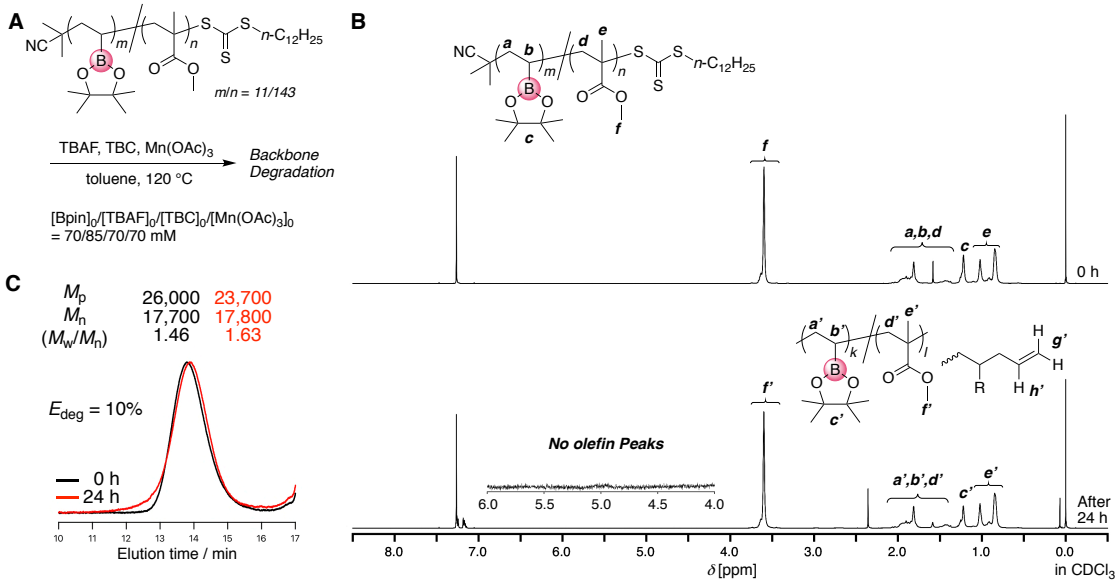

Figure S5. (A) Reaction condition for the degradation of poly(VBpin-*co*-MMA) (run 2 in Table 1). (B) ^{1}H NMR spectra of the precursor (upper) and the resultant polymer (bottom). (C) SEC traces of the precursor (black) and the resultant polymer (red).

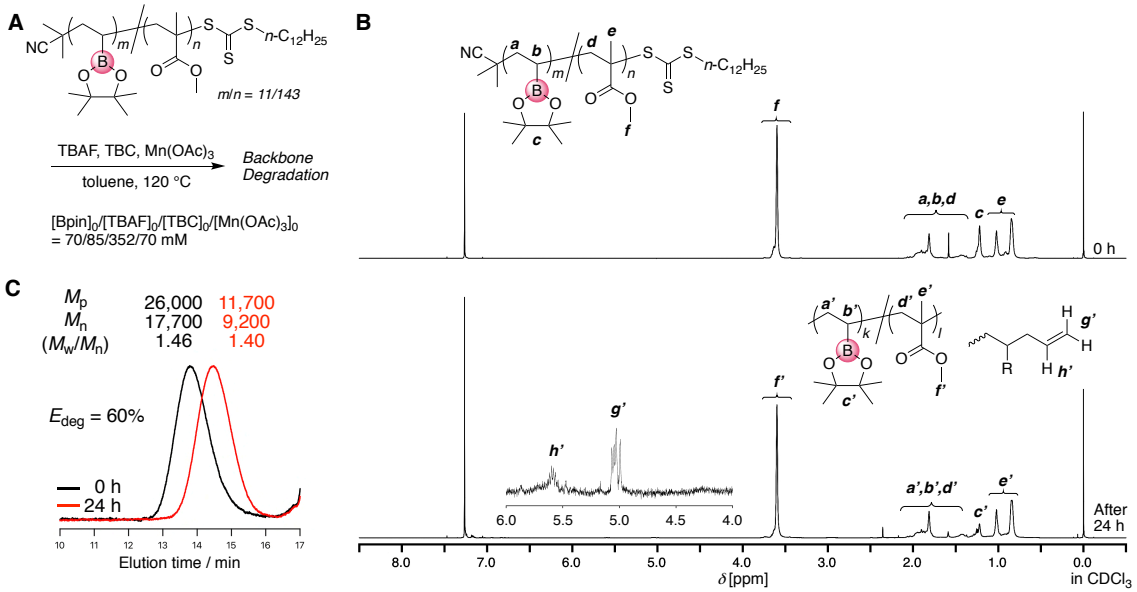

Figure S6. (A) Reaction condition for the degradation of poly(VBpin-*co*-MMA) (run 3 in Table 1). (B) ^{1}H NMR spectra of the precursor (upper) and the resultant polymer (bottom). (C) SEC traces of the precursor (black) and the resultant polymer (red).

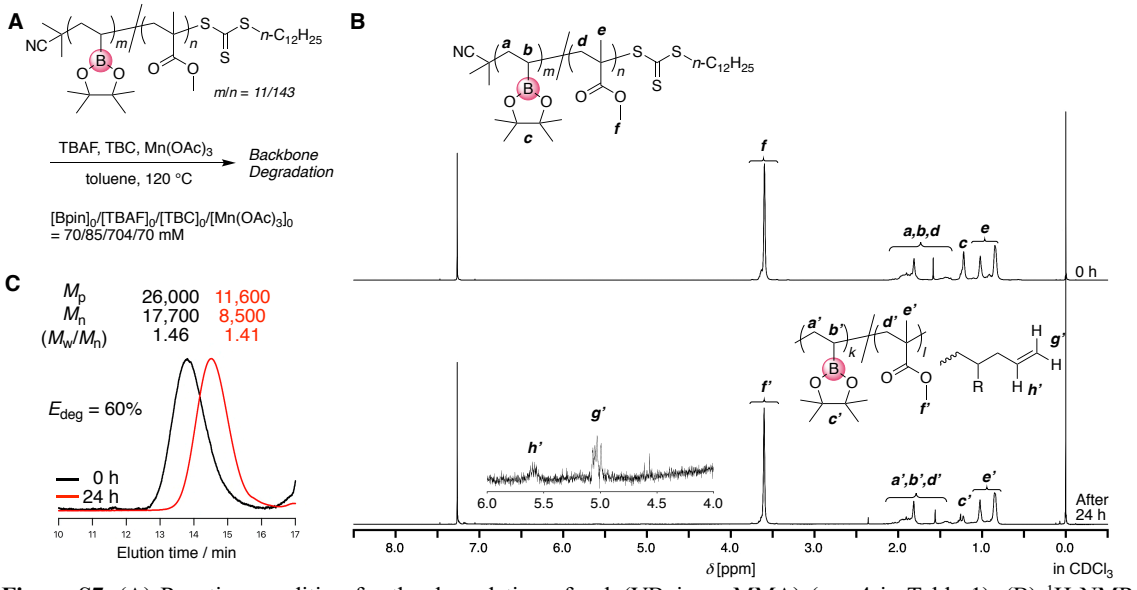

Figure S7. (A) Reaction condition for the degradation of poly(VBpin-*co*-MMA) (run 4 in Table 1). (B) ^{1}H NMR spectra of the precursor (upper) and the resultant polymer (bottom). (C) SEC traces of the precursor (black) and the resultant polymer (red).

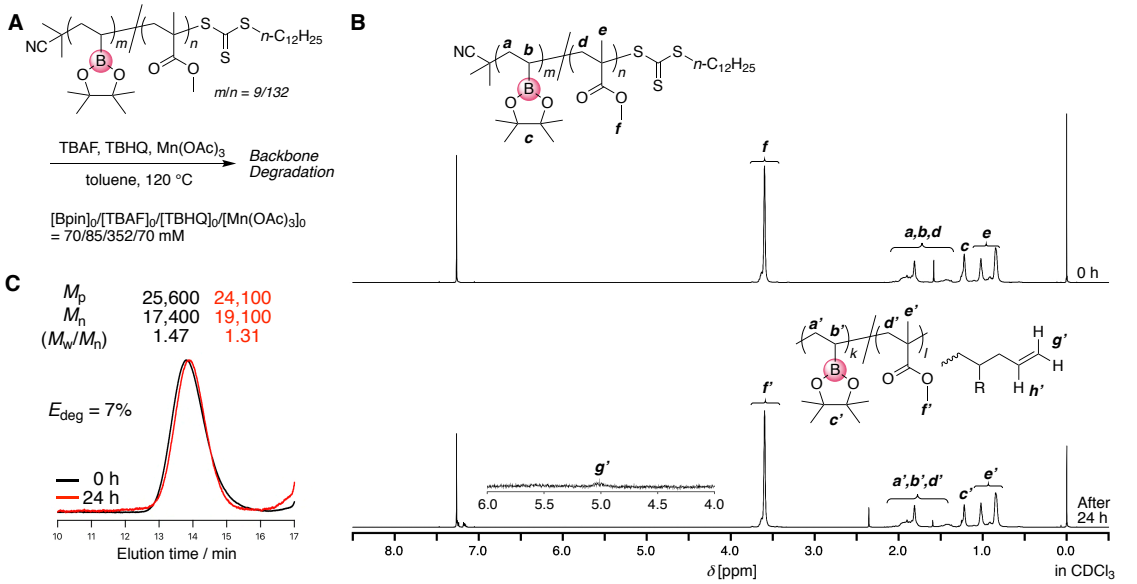

Figure S8. (A) Reaction condition for the degradation of poly(VBpin-*co*-MMA) (run 5 in Table 1). (B) ^{1}H NMR spectra of the precursor (upper) and the resultant polymer (bottom). (C) SEC traces of the precursor (black) and the resultant polymer (red).

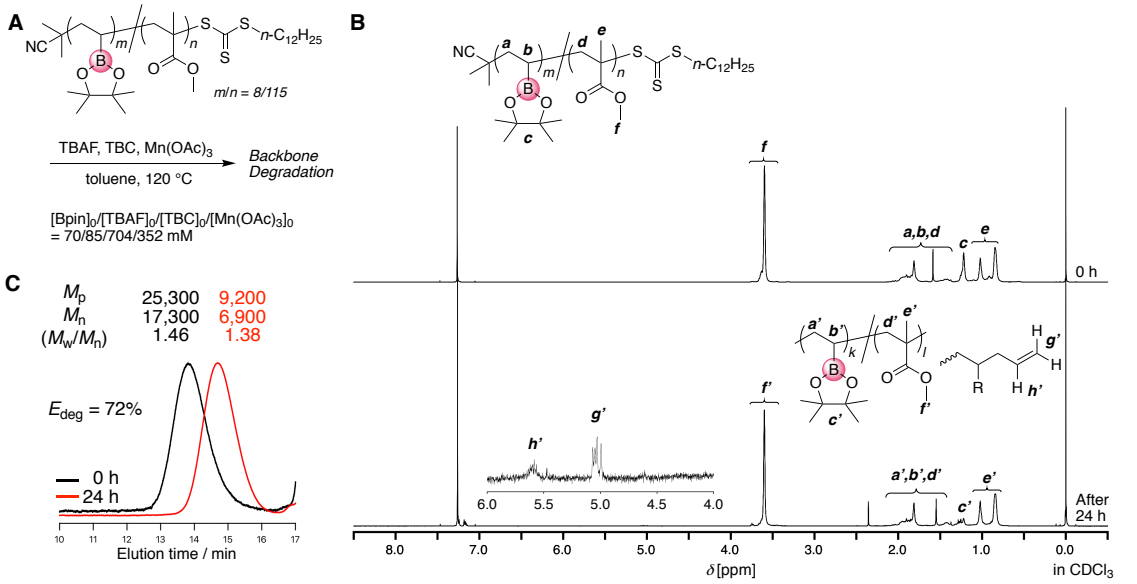

Figure S9. (A) Reaction condition for the degradation of poly(VBpin-*co*-MMA) (run 6 in Table 1). (B) ^{1}H NMR spectra of the precursor (upper) and the resultant polymer (bottom). (C) SEC traces of the precursor (black) and the resultant polymer (red).

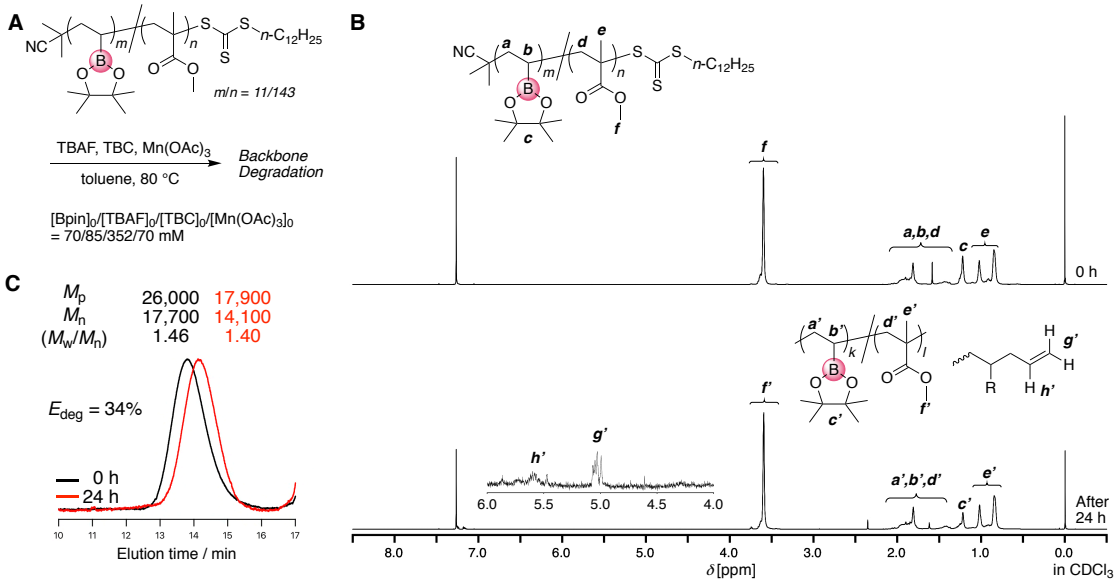

Figure S10. (A) Reaction condition for the degradation of poly(VBpin-*co*-MMA) at 80 °C. (B) ^{1}H NMR spectra of the precursor (upper) and the resultant polymer (bottom). (C) SEC traces of the precursor (black) and the resultant polymer (red).

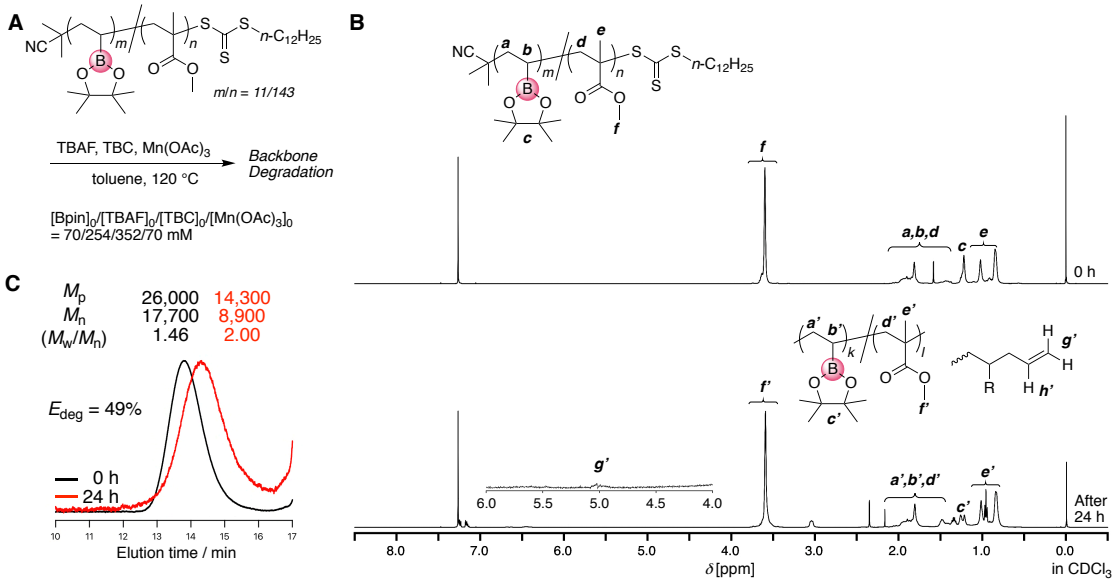

Figure S11. (A) Reaction condition for the degradation of poly(VBpin-*co*-MMA) with TBAF (3.6 eq.). (B) ^{1}H NMR spectra of the precursor (upper) and the resultant polymer (bottom). (C) SEC traces of the precursor (black) and the resultant polymer (red).

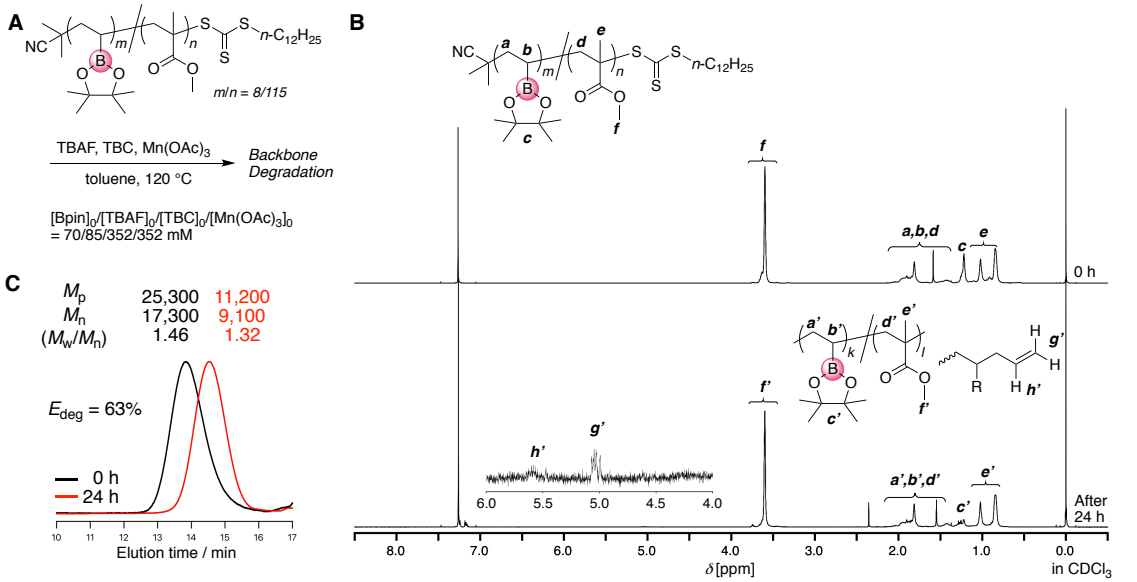

Figure S12. (A) Reaction condition for the degradation of poly(VBpin-*co*-MMA) with $Mn(OAc)_3$ (5.0 eq.). (B) ^1H NMR spectra of the precursor (upper) and the resultant polymer (bottom). (C) SEC traces of the precursor (black) and the resultant polymer (red).

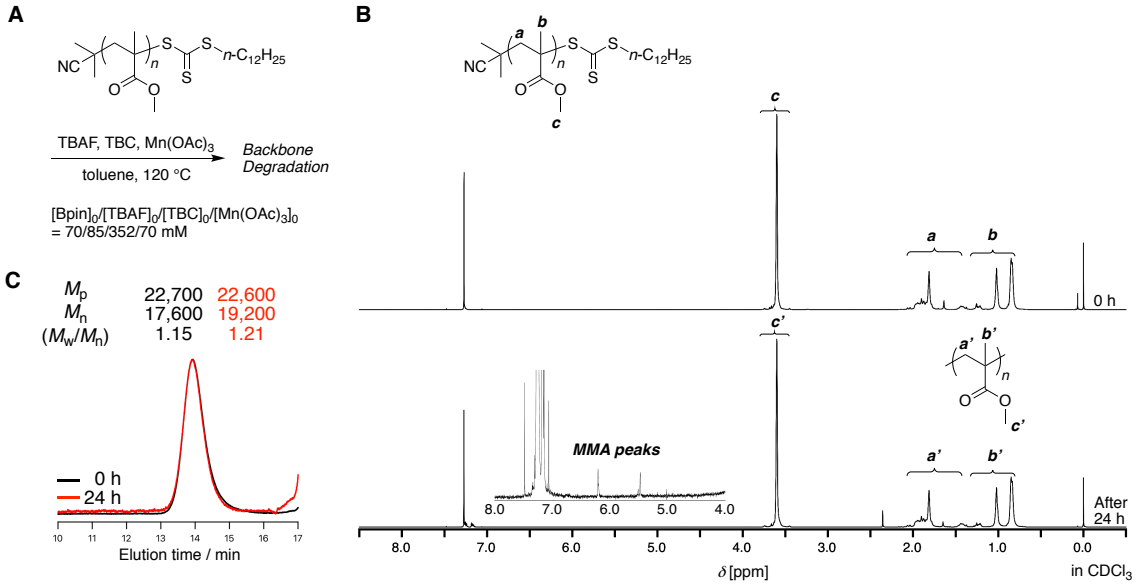

Figure S13. (A) Reaction condition for the degradation of PMMA (Figure 2C). (B) ^1H NMR spectra of the precursor (upper) and the resultant polymer (bottom). (C) SEC traces of the precursor (black) and the resultant polymer (red).

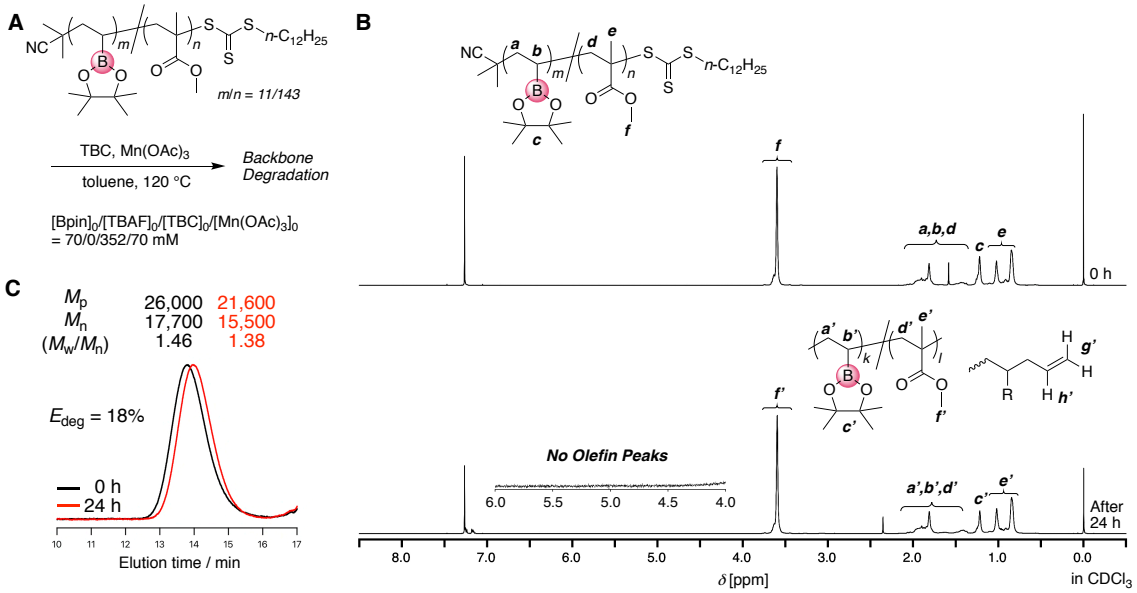

Figure S14. (A) Reaction condition for the degradation of poly(VBpin-*co*-MMA) (Figure 2D). (B) ^{1}H NMR spectra of the precursor (upper) and the resultant polymer (bottom). (C) SEC traces of the precursor (black) and the resultant polymer (red).

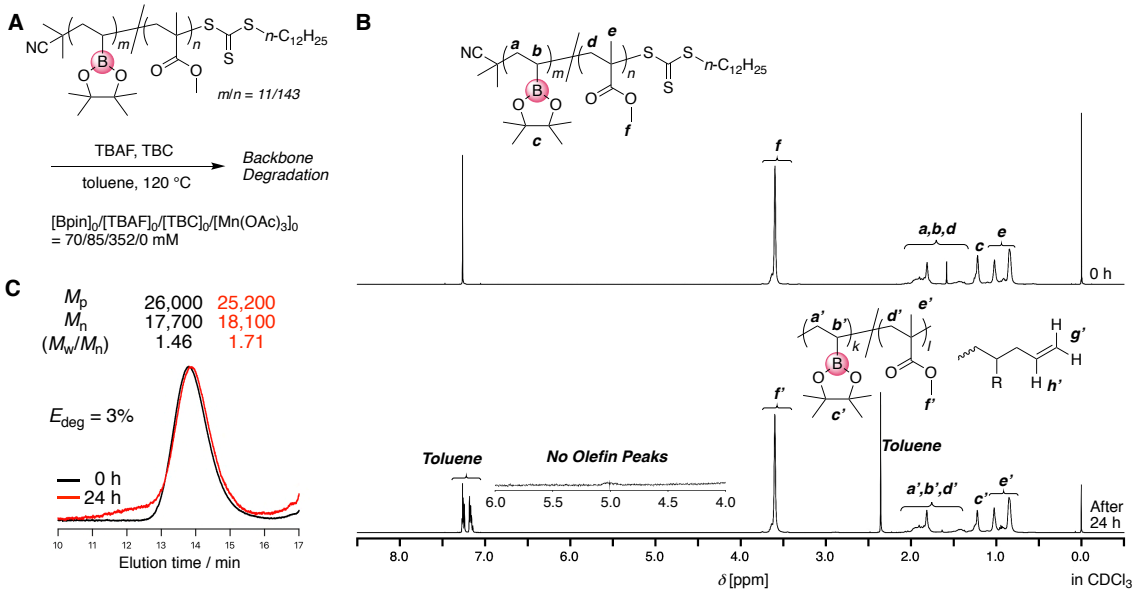

Figure S15. (A) Reaction condition for the degradation of poly(VBpin-*co*-MMA) (Figure 2E). (B) ^{1}H NMR spectra of the precursor (upper) and the resultant polymer (bottom). (C) SEC traces of the precursor (black) and the resultant polymer (red).

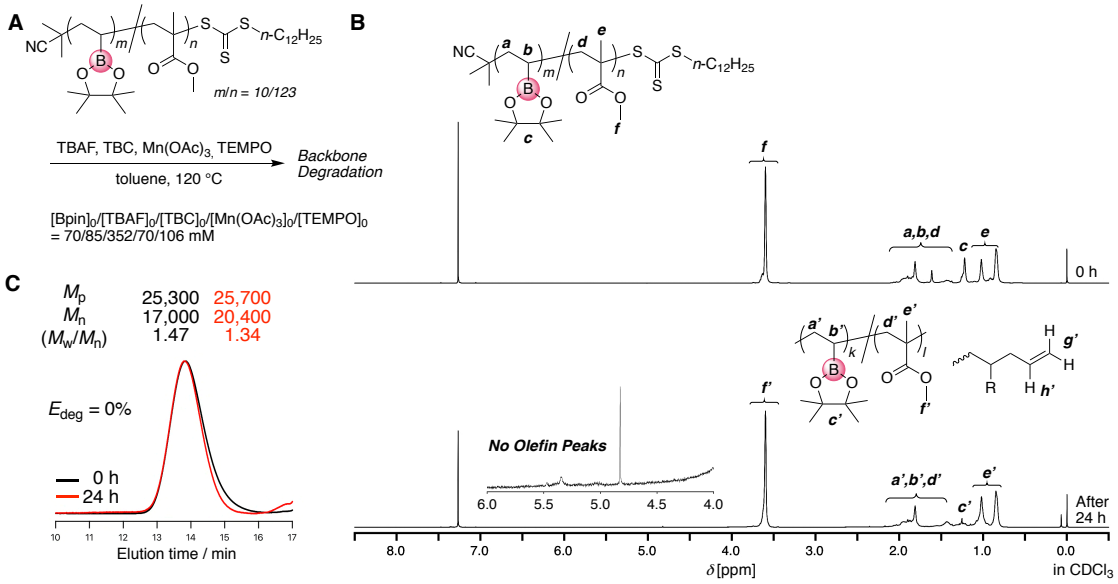

Figure S16. (A) Reaction condition for the degradation of poly(VBpin-*co*-MMA) (Figure 2F). (B) ^{1}H NMR spectra of the precursor (upper) and the resultant polymer (bottom). (C) SEC traces of the precursor (black) and the resultant polymer (red).

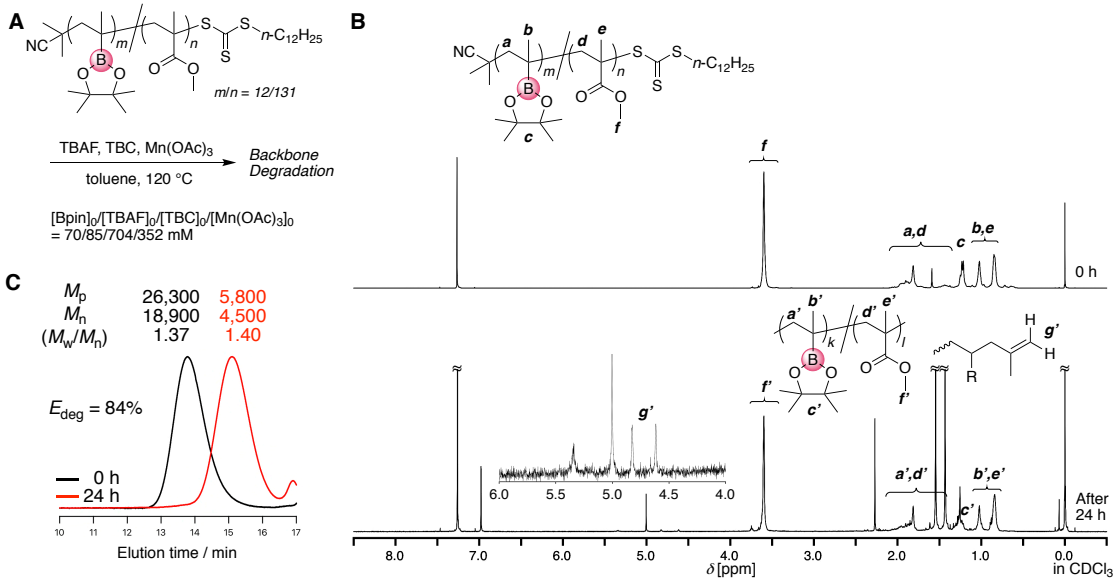

Figure S17. (A) Reaction condition for the degradation of poly(IPBpin-*co*-MMA) (Figure 3C). (B) ^{1}H NMR spectra of the precursor (upper) and the resultant polymer (bottom). (C) SEC traces of the precursor (black) and the resultant polymer (red).

5 Thermal Properties of Obtained Polymers

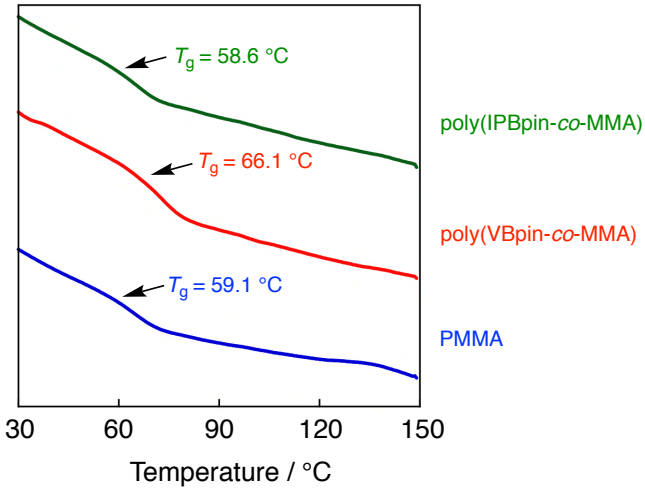

Figure S18. DSC curves of poly(IPBpin-*co*-MMA) (M_n = 18,600, M_w/M_n = 1.36, IPBpin = 9.6%), poly(VBpin-*co*-MMA) (M_n = 17,700, M_w/M_n = 1.46, VBpin = 7.4%), and PMMA (M_n = 17,600, M_w/M_n = 1.15).

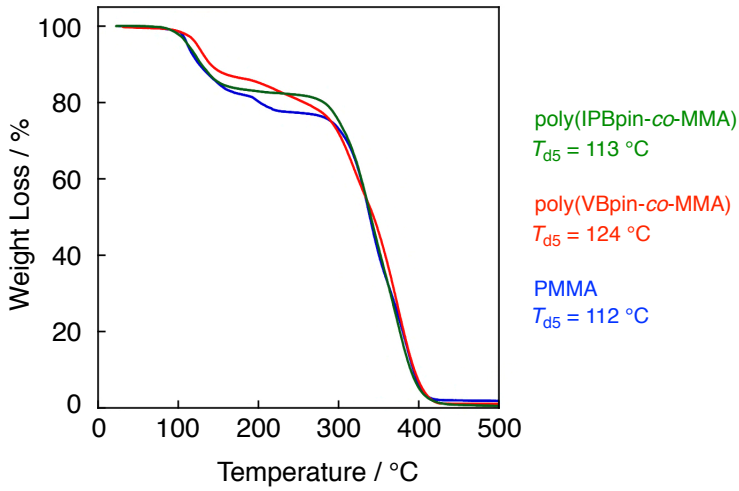

Figure S19. TGA curves of poly(IPBpin-*co*-MMA) (M_n = 18,600, M_w/M_n = 1.36, IPBpin = 9.6%), poly(VBpin-*co*-MMA) (M_n = 17,700, M_w/M_n = 1.46, VBpin = 7.4%), and PMMA (M_n = 17,600, M_w/M_n = 1.15).